Yap Controls Stem/Progenitor Cell Proliferation in the Mouse Postnatal Epidermis

Annemiek Beverdam[1], Christina Claxton[1], Xiaomeng Zhang[2,3,4], Gregory James[1], Kieran F. Harvey[2,3,4] and Brian Key[1]

Tissue renewal is an ongoing process in the epithelium of the skin. We have begun to examine the genetic mechanisms that control stem/progenitor cell activation in the postnatal epidermis. The conserved Hippo pathway regulates stem cell turnover in arthropods through to vertebrates. Here we show that its downstream effector, yes-associated protein (YAP), is active in the stem/progenitor cells of the postnatal epidermis. Overexpression of a C-terminally truncated YAP mutant in the basal epidermis of transgenic mice caused marked expansion of epidermal stem/progenitor cell populations. Our data suggest that the C-terminus of YAP controls the balance between stem/progenitor cell proliferation and differentiation in the postnatal interfollicular epidermis. We conclude that YAP functions as a molecular switch of stem/progenitor cell activation in the epidermis. Moreover, our results highlight YAP as a possible therapeutic target for diseases such as skin cancer, psoriasis, and epidermolysis bullosa.

Journal of Investigative Dermatology (2013) **133,** 1497–1505; doi:10.1038/jid.2012.430; published online 29 November 2012

INTRODUCTION

Perturbations to epidermal basal stem/progenitor proliferation result in unbalanced epidermal homeostasis and devastating diseases such as skin cancer, psoriasis, and epidermolysis bullosa. yes-associated protein (YAP) has been identified in a transcriptional profiling screen as a ''stemness'' gene (Ramalho-Santos *et al.*, 2002). It is a transcriptional coactivator that is regulated by the highly conserved Hippo pathway to control tissue homeostasis (Harvey and Tapon, 2007). In mammals, the core of this pathway consists of several negative growth regulators acting in a kinase cascade, including MST1/2 and its regulatory protein SAV, which ultimately phosphorylates YAP serine residue 127 (S127-phospho-YAP), causing inactivation through cytoplasmic retention (Dong *et al.*, 2007). Unphosphorylated YAP translocates to the nucleus where it interacts with the TEAD transcription factors to activate target gene transcription and cell proliferation (Ota and Sasaki, 2008; Wu *et al.*, 2008; Zhang *et al.*, 2008b; Zhao *et al.*, 2008).

[1]*School for Biomedical Sciences, The University of Queensland, Brisbane, Queensland, Australia;* [2]*Cell Growth and Proliferation Laboratory, Peter MacCallum Cancer Centre, East Melbourne, Victoria, Australia;* [3]*Sir Peter MacCallum Department of Oncology, University of Melbourne, Parkville, Victoria, Australia and* [4]*Department of Pathology, University of Melbourne, Parkville, Victoria, Australia*

Correspondence: Annemiek Beverdam, or Brian Key, School for Biomedical Sciences, The University of Queensland, Brisbane, Queensland, Australia. E-mail: a.beverdam@uq.edu.au or brian.key@uq.edu.au

Abbreviations: Gli2, glioma-associated oncogene family zinc finger 2; YAP, yes-associated protein

Received 29 November 2011; revised 5 September 2012; accepted 17 September 2012; published online 29 November 2012

Gain- and loss-of-function mice have shown that the Hippo pathway and *Yap* are critical regulators of organ size *in vivo* (Camargo *et al.*, 2007; Dong *et al.*, 2007; Zhou *et al.*, 2009; Lu *et al.*, 2010; Song *et al.*, 2010; Schlegelmilch *et al.*, 2011; Zhang *et al.*, 2011a; Zhou *et al.*, 2011). Deregulation of Hippo/YAP signaling has been implicated in tumorigenesis, and *Yap* is generally considered to be a potent oncogene in both mice and humans (reviewed by Chan *et al.*, 2011). Interestingly, high nuclear YAP expression in human cancer was shown to correlate with poor prognosis (Xu *et al.*, 2009; Hall *et al.*, 2010; Wang *et al.*, 2010; Zhang *et al.*, 2011b).

We have overexpressed a mutant form of YAP in transgenic mice to examine the function of this ''stemness'' gene specifically in epidermal homeostasis. We found a severe expansion of the epidermal stem/progenitor cell compartments and progressive postnatal alopecia that involved coat and whiskers. Our data support a role of YAP in epidermal stem/progenitor cell proliferation through regions in its N-terminus, including the TEAD-binding domain. In contrast, the balance between proliferation and differentiation in the interfollicular epidermis appears to be dependent on the C-terminal YAP regions, including YAP transactivation domain. We conclude that YAP is a key regulator that lies at the crossroads of proliferation, differentiation, and homeostatic maintenance in the pathway controlling the cytoarchitecture of epidermis.

RESULTS AND DISCUSSION

YAP is expressed in proliferative zones of the skin

Initially, we investigated YAP expression in the epidermis of wild-type mice (at postnatal day 85, P85; Figure 1). Using a pan-YAP antibody, we detected prominent YAP expression in the bulge of the proximal hair follicle and in the interfollicular

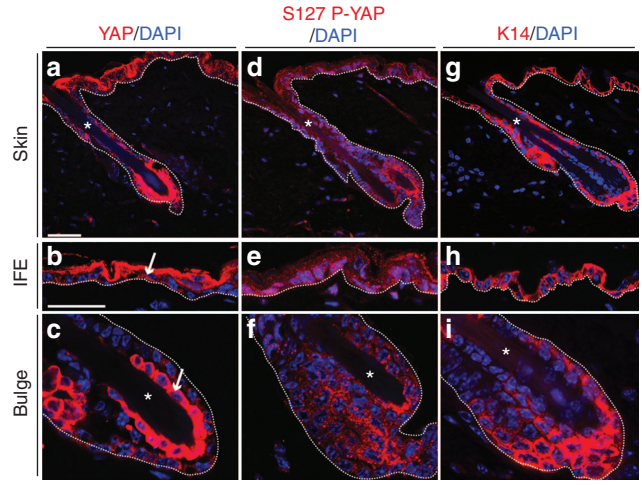

Figure 1. YAP is expressed in the proliferative zones of the epidermis. (**a**–**i**) Immunofluoresence staining in sections through the dorsal skin of P89 wild-type mice detecting pan-YAP (**a**–**c**), phospho-Serine127 YAP (P-YAP) (**d**–**f**), and basal cell marker Keratin 14 (**g**–**i**). Arrows point at YAP expression in basal cells in **b** and in bulge cells in **c**. Asterisks mark hair shafts. Basement membranes are demarcated by dashed lines. DAPI, 4′,6-diamidino-2-phenylindole; IFE, interfollicular epidermis; YAP, yes-associated protein. Scale bars = 100 μm.

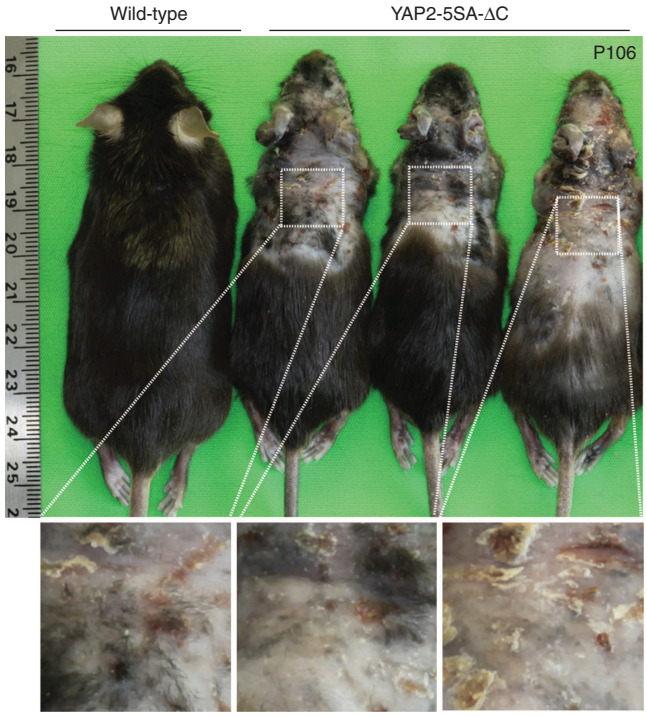

Figure 2. Progressive dorsal alopecia in YAP2-5SA-ΔC transgenic mice. 1x wild-type (left) and 3x YAP2-5SA-ΔC transgenic (right) P106 littermates. Note that transgenic animals display alopecia and loss of whiskers. Affected regions of dorsal skin of each transgenic mouse are magnified and displayed at bottom of the figure.

epidermis (Figure 1a). YAP was clearly detected in the cytoplasm of basal cells in the interfollicular epidermis and in the bulge (arrows, Figure 1b–c). A similar expression pattern was observed for S127-phosphorylated YAP (Figure 1d–f), providing evidence that the Hippo pathway was functional in these cells to control YAP activity. Both antibodies revealed that YAP was present at relatively low levels along the outer root sheaths of hair follicles and at high levels in the bulge regions. The expression was mostly localized to the cytosol, consistent with recent reports of the reduced nuclear localization of YAP in skin during the perinatal period (Zhang *et al.*, 2011a). Immunostaining for the intermediate filament protein Keratin 14, a marker of bulge and basal epidermal cells (Fuchs and Green, 1980), was very similar to the YAP expression pattern in the skin (Figure 1g–i). Together, this immunostaining expression data suggest that the Hippo pathway and YAP may have a role in postnatal epidermal tissue homeostasis.

Manipulating YAP activity perturbs skin maturation

We next manipulated endogenous YAP activity in the epidermis *in vivo* by transgenesis. We exploited a previously generated mutant YAP protein ''YAP2-5SA-ΔC'' that is insensitive to the Hippo pathway–induced cytoplasmic localization because it lacks the serine residues, which are normally phosphorylated (Hoshino *et al.*, 2006; Zhao *et al.*, 2007). This YAP variant also lacks region C-terminal from Q281, including a transactivation domain, which prevents it from activating gene expression *in vitro*. YAP2-5SA-ΔC was forcibly expressed in the basal stem/progenitor cells of the epidermis in transgenic mice from 13.5 dpc onward (shortly after the onset of epidermal stratification), using a bovine *Keratin 5* promoter fragment (Ramirez *et al.*, 1994). We anticipated that this mutant protein would block endogenous YAP function and disrupt tissue homeostasis. We obtained five independent YAP2-5SA-ΔC transgenic mouse lines displaying identical epidermal phenotypes. Quantitative real-time PCR assays confirmed high expression levels of the transgene in the skin of P85 YAP2-5SA-ΔC transgenic mice, whereas endogenous *Yap* expression levels were not different from wild-type skin.

Newborn YAP2-5SA-ΔC transgenic mice were healthy and grossly indistinguishable from their wild-type littermates. At P7, although the skin of YAP2-5SA-ΔC transgenic mice became dry and scaly, their pelage developed similarly to that of wild-type littermates. From 4–5 weeks of age, coinciding with the second postnatal anagen phase (Muller-Rover *et al.*, 1999), the transgenic mice developed progressive dorsal alopecia usually starting dorsally and gradually spreading out across the body and resulting in complete baldness. The transgenic mice also lost many of their whiskers (P106 wild-type and transgenic littermates shown in Figure 2). The affected skin regions were very dry and lost pliability. Skin lesions developed, possibly because of excessive scratching, but usually healed very rapidly (boxed inserts, Figure 2). Despite this abnormal skin phenotype, we did not observe any clear signs of tumor formation in the epidermis of transgenic mice up to 1 year of age.

Altered skin histogenesis in YAP2-5SA-ΔC transgenic mice

The histology of newborn YAP2-5SA-ΔC transgenic epidermis appeared similar in comparison with wild-type animals (Figure 3a and b). However, Keratin 14 immunostaining

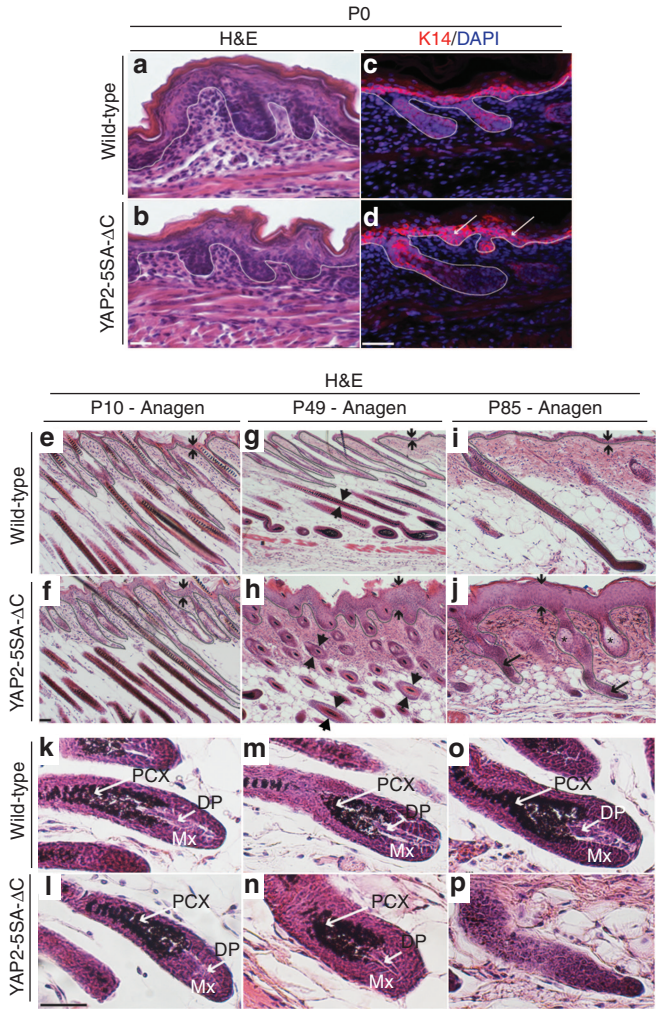

Figure 3. Ontology of the epidermal phenotype in YAP2-5SA-ΔC transgenic mice. H&E (**a**, **b**, **e–p**) and Keratin 14 immunostaining assays (**c**, **d**) of wild-type (**a**, **c**, **e**, **g**, **i**, **k**, **m**, **o**) and YAP2-5SA-ΔC transgenic (**b**, **d**, **f**, **h**, **j**, **l**, **n**, **p**) skin of P0 (**a–d**), P10 (**e**, **f**, **k**, **l**), P49 (**g**, **h**, **m**, **n**), and P85 (**i**, **j**, **o**, **p**) littermates. Single white arrows in **d** point at irregularities in the basal layer of P0 YAP2-5SA-ΔC transgenic epidermis. Opposing arrows in **e–j** highlight thickness of the interfollicular epidermis. Opposing arrowheads in **g**, **h** highlight the thickness of the hair follicle shaft. Single arrows in **j** point at expanded cell masses in hair follicles of P85 YAP2-5SA-ΔC transgenic skin. Asterisks in **j** mark enlarged sebaceous glands. Basement membranes are demarcated by dashed lines. DAPI, 4′,6-diamidino-2-phenylindole; DP, dermal papilla; H&E, hematoxylin and eosin staining; Mx, matrix; PCX, precortex. Scale bars = 100 μm.

revealed initial signs of regional irregularities in the thickness of the basal stem/progenitor cell layer of the transgenic interfollicular epidermis (arrows, Figure 3d and 3c). At P10, during the first postnatal anagen phase, we detected local thickenings of the interfollicular epidermis (opposing arrows in Figure 3F with similar region in Figure 3e). The hair follicles at this age appeared similar in control and transgenic animals (dotted outlines, Figure 3e and f). There was no discernable difference in the histological appearance of the dermal papilla, matrix, or precortex in the hair bulb (Figure 3k and l). At P49, shortly after the onset of hair loss in transgenic mice, both the interfollicular epidermis (opposing arrows in Figure 3h) and the outer root sheaths were clearly thicker (opposing arrows in Figure 3g and h), whereas the hair bulbs were relatively normal (Figure 3m and n). By P85, the interfollicular epidermis of YAP2-5SA-ΔC transgenic mice was now markedly thickened (Figure 3i and j; also see thickness increase between Figure 3f, 3h, and 3j). Moreover, the sebaceous glands in hair follicles were grossly enlarged (asterisks in Figure 3j). Hair follicles in YAP2-5SA-ΔC adult mice did appear to undergo anagen, although the cycling proximal hair follicles extended highly abnormal rudimentary cell masses into the dermis (single arrows in Figure 3j), which lacked hair shafts or obvious signs of hair bulb structures such as the dermal papillae or matrix cells (Figure 3o and p). This aberrant morphology probably accounts for the alopecia in transgenic animals.

Next, we examined the cellular constituency of the interfollicular epidermis of P85 wild-type and YAP2-5SA-ΔC littermates in more detail. Immunostaining revealed a marked expansion of the Keratin 14–expressing basal cell populations in the interfollicular epidermis and hair follicles of transgenic mice (Figure 4a and b). The Keratin 10–expressing spinous layer (Figure 4c and d) and involucrin-expressing granular layer (Figure 4e and f) also had clearly thickened in transgenic animals compared with wild-type animals. In addition, loricrin staining revealed a thickening of the cornified layer, indicative of hyperkeratinization in the transgenic animals (Figure 3g and h). To assess whether cell proliferation patterns in the epidermis were affected by expression of the transgene, we immunostained tissue sections for the expression of the mitosis marker phospho-histone H3 (Hans and Dimitrov, 2001). Only small numbers of dividing nuclei were present in the basal layer of the wild-type interfollicular epidermis, whereas large numbers of dividing nuclei were detected throughout both basal and suprabasal layers of the YAP2-5SA-ΔC interfollicular epidermis (arrows in Figure 3i and j). We counted mitotic nuclei and found ~20-fold higher numbers of proliferating cells in the YAP2-5SA-ΔC transgenic epidermis compared with wild-type P85 epidermis ($n = 3$, data not shown). To assess the identity of these dividing cells, we performed immunostaining assays with epidermal progenitor cell marker, P63 (Hans and Dimitrov, 2001), and found that in wild-type epidermis, the progenitor cells were typically localized to the basal layer of the interfollicular epidermis (arrows, Figure 3k). In contrast, the P63-expressing progenitor cell population had expanded and was now clearly present in both basal and suprabasal layers in the YAP2-5SA-ΔC interfollicular epidermis (arrows, Figure 3l). Together, these data suggest that the overexpression of YAP2-5SA-ΔC in postnatal epidermis resulted in hyperproliferation of the basal stem/progenitor cell population and an expansion of the principal cell layers of the interfollicular epidermis.

Next, we turned our attention to the cellular constituency of the P85 anagen hair follicles. In wild-type follicles, Keratin 14 is discretely expressed in the outer root sheath cells that surround the hair shaft (Figure 5a). In the absence of the hair shaft in transgenic animals, the Keratin 14–expressing cell populations appear to have expanded and form an elongated

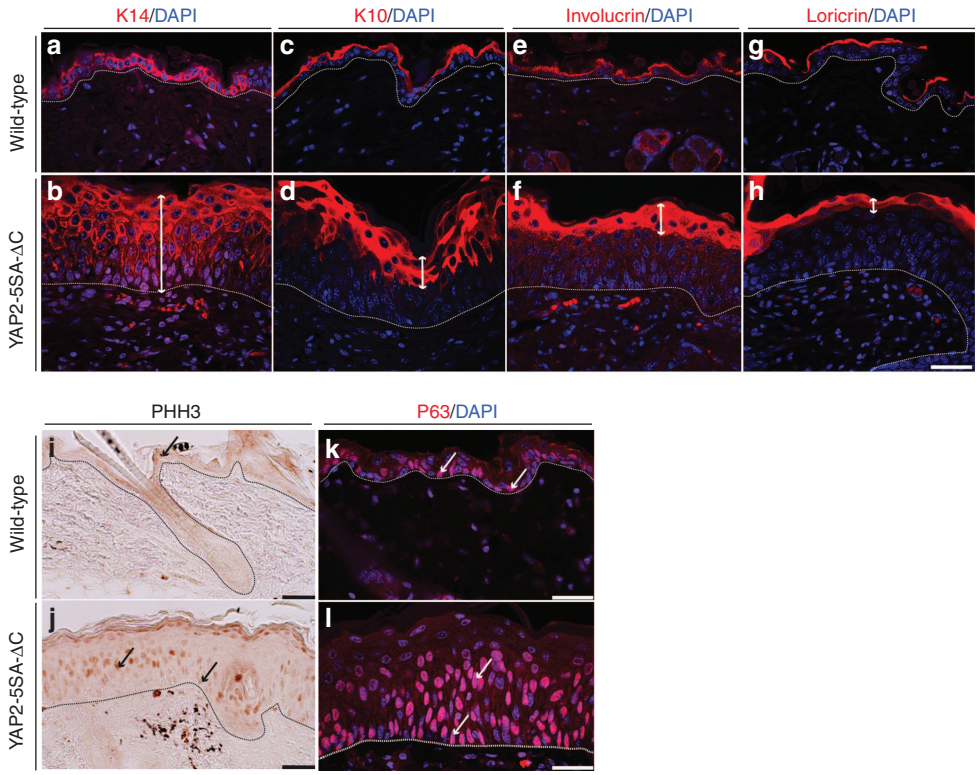

Figure 4. Expansion of basal stem/progenitor cells and suprabasal layers in the interfollicular epidermis of YAP2-5SA-ΔC transgenic mice. Immunostaining assays on sections of wild-type (**a**, **c**, **e**, **g**, **i**, **k**) and YAP2-5SA-ΔC transgenic (**b**, **d**, **f**, **h**, **j**, **l**) skin of P85 littermates showing the expression of basal marker K14 (**a**, **b**), spinous cell marker K10 (**c**, **d**), granular cell marker involucrin (**e**, **f**), cornified layer marker loricrin (**g**, **h**), proliferation marker PHH3 (**i**, **j**), and basal stem/progenitor cell marker P63 (**k**, **l**). Double arrows in **b, d, f, h** highlight thickness of the relevant epidermal layers. Arrows in **i, j** indicate proliferating cells. Arrows in **k**, **l** indicate P63-expressing nuclei. Basement membranes are demarcated by dashed lines. DAPI, 4′,6-diamidino-2-phenylindole; PHH3, phospho-histone H3. Scale bars = 100 μm.

and irregular-shaped tail or strand of cells (arrows in Figure 5b). The expression of Keratin 6 is usually restricted to the companion layer of the hair follicles (Figure 5c), and it is upregulated in hyperproliferative epidermal cells (Winter *et al.*, 1998). We could not identify Keratin 6 expression reminiscent of the companion layer in the interfollicular epidermis of the YAP2-5SA-ΔC transgenic mice, but it was highly expressed in discrete proliferative cell masses in the hair follicles (arrows in Figure 5d and f), as well as in the suprainfundibular hair shafts and interfollicular epidermis of the YAP2-5SA-ΔC transgenic mice (above dashed lines in Figure 5d), consistent with the increased cell proliferation previously shown (Figure 4j). Interestingly, the proliferative cell masses located in the abnormal proximal hair follicles also expressed hair follicle bulge stem/progenitor cell markers Keratin 15 (Figure 5g with Figure 5h; Liu *et al.*, 2003), SOX9 (Figure 5i with Figure 5j; Vidal *et al.*, 2005), LHX2 (Figure 5k with Figure 5l; Rhee *et al.*, 2006), and CD34 (Figure 5m with Figure 5n; Trempus *et al.*, 2003). These data show that the bulge stem/progenitor cell populations have markedly expanded in the YAP2-5SA-ΔC transgenic mice.

Next, we wanted to determine whether the hair germ was present in the hair follicles of the P85 YAP2-5SA-ΔC transgenic mice. The hair germ is a transient structure present between the dermal papilla and hair follicle bulge during late catagen/telogen and is thought to be populated by hair follicle bulge stem/progenitor cells (Chase *et al.*, 1951; Panteleyev *et al.*, 2001; Ito *et al.*, 2004; Schmidt-Ullrich and Paus, 2005; Greco *et al.*, 2009). We performed co-immunostaining assays with antibodies against P-Cadherin, which is highly expressed in the hair germ and in the hair follicle bulge in late catagen/telogen hair follicles (Muller-Rover *et al.*, 1999; Greco *et al.*, 2009), and CD34, which exclusively marks hair follicle bulge stem/progenitor cells and not hair germ cells (Trempus *et al.*, 2003; Greco *et al.*, 2009). In P85 wild-type mice, we detected P-Cadherin at high levels in the hair germ and in the bulge of late telogen/catagen hair follicles, whereas CD34 was exclusively expressed in the hair follicle bulge (Figure 5o), which is consistent with previous reports (Muller-Rover *et al.*, 1999; Trempus *et al.*, 2003; Greco *et al.*, 2009). In contrast, in the expanded proximal hair follicles of the YAP2-5SA-ΔC transgenic mice, CD34 expression fully overlapped with that of P-Cadherin (yellow signal in Figure 5p). Altogether, these data suggest that the expanded proximal hair follicles of the YAP2-5SA-ΔC transgenic mice exclusively consist of bulge stem/progenitor cells and lack hair germ cells.

To determine whether hair follicle bulge stem/progenitor cells produced matrix cells, hair shaft, and inner root sheath in YAP2-5SA-ΔC transgenic mice, we performed quantitative real-time PCR assays and found strongly reduced expression

levels of hair matrix markers *Lef1* and *Msx2* in the P85 YAP2-5SA-ΔC transgenic epidermis ($P<0.05$; $n=3$, Figure 5q; Reginelli *et al.*, 1995; Zhou *et al.*, 1995). In addition, differentiation markers of the hair shaft (AE13) and inner root sheath (trichohyalin, AE15) were strongly reduced at P49 ($P<0.05$; $n=3$, Figure 5q) and undetectable at P85 ($P<0.05$; $n=3$, data not shown) in the skins of YAP2-5SA-ΔC transgenic mice, demonstrating complete loss of hair follicle differentiation, consistent with the observed alopecia (Figure 3j).

Finally, we wanted to investigate whether the dermal papilla, which controls hair cycle activation (Gat *et al.*, 1998; Van Mater *et al.*, 2003; Lo Celso *et al.*, 2004; Lowry *et al.*, 2005; Rendl *et al.*, 2008; Zhang *et al.*, 2008c), had a role in the observed abnormalities. Alkaline phosphatase staining was used to depict dermal papilla in the epidermis from animals at P10, P49, and P85 (Figure 5t–y). Though the dermal papillae were present at P85 at the proximal tip of the abnormal hair follicles, these structures were not enveloped by the matrix cells, as in either wild-type littermates or at earlier developmental stages (Figure 5w with Figure 5r–v). These results suggest that it is not the lack of the dermal papillae but rather, perhaps, the aberrant signaling from this center that underlies the abnormal growth pattern of the hair follicle in the P85 YAP2-5SA-ΔC transgenic mice.

The C-terminus of YAP is dispensable for cell proliferation *in vivo*

Interestingly, the changes in skin morphology in our YAP2-5SA-ΔC postnatal mice seem to represent a ''gain-of-function'' rather than a ''loss-of-function'' phenotype, as we had anticipated on the basis of *in vitro* results previously obtained with this mutant YAP (Hoshino *et al.*, 2006; Zhao *et al.*, 2007). Indeed, the hyperproliferative phenotype of the basal and suprabasal epidermal stem/progenitor cell populations that we observed with the overexpression of YAP2-5SA-ΔC was also reported in lines of inducible transgenic mice, in which a constitutively active full-length YAP mutant (YAPS127A) was expressed in the progenitor cell population of the epidermis (Schlegelmilch *et al.*, 2011; Zhang *et al.*, 2011a). In contrast, conditional mutant mice that either lack the *Yap* gene or express a YAP(S79A) mutant, which is incapable of binding TEAD cofactors in the epidermis, display a severely thinned

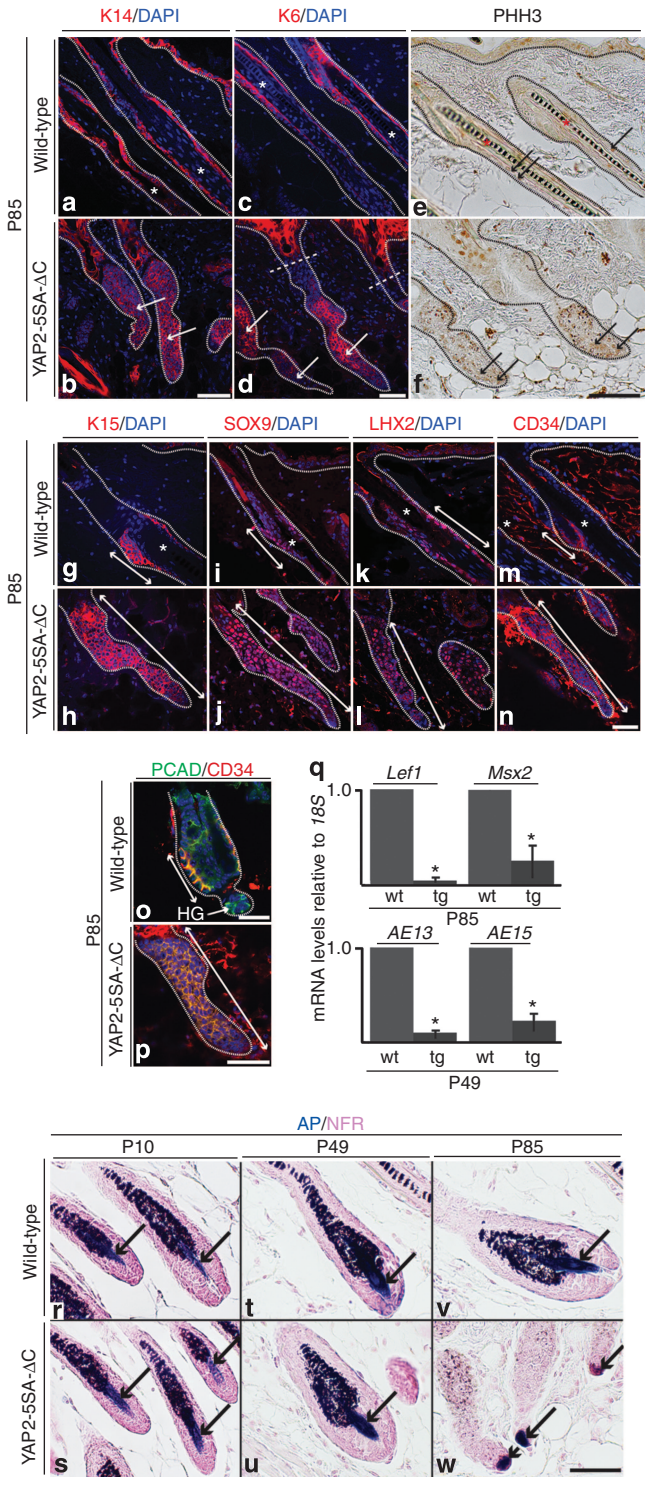

Figure 5. Expansion of hair follicle bulge stem/progenitor cell population in YAP2-5SA-ΔC transgenic mice. Immunostaining (**a**–**p**), quantitative real-time reverse transcriptase–PCR (**q**), and alkaline phosphatase staining assays (**r**–**w**) on the epidermis of wild-type and YAP2-5SA-ΔC transgenic littermates showing the expression of outer root sheath marker Keratin 14 (**a**, **b**), companion layer marker K6 (**c**, **d**), proliferation marker PHH3 (**e**, **f**), bulge stem/progenitor cell markers K15 (**g**, **h**), SOX9 (**i**, **j**), LHX2 (**k**, **l**), and CD34 (**m**, **n**), P-Cadherin and CD34 (**o**, **p**), and the location of the dermal papilla (**r**–**w**). (**q**) Quantitative real-time reverse transcriptase–PCR assays show the expression levels of hair matrix markers *Lef1* and *Msx2*, inner root sheath marker *AE13*, and hair shaft marker *AE15* in the epidermis of wild-type and YAP2-5SA-ΔC transgenic littermates. Arrows in **e**, **f** indicate dividing cells. Double arrows in **g**–**b** highlight size of the hair follicle bulge region. Arrow in **o** indicates the hair germ. (**q**) y Axis displays relative fold expression levels with the expression levels in wild-type set to 1. Error bars represent mean ± SEM ($N=3$). Asterisks indicate statistically significant differences in gene expression levels ($P<0.05$). Arrows in **r**–**w** indicate location of the dermal papilla. Asterisk mark hair shafts. Basement membranes are demarcated by dashed lines. AP, alkaline phosphatase; DAPI, 4′,6-diamidino-2-phenylindole; mRNA, messenger RNA; NFR, nuclear fast red; PCAD, P-Cadherin; PHH3, phosphohistone H3; tg, transgenic; wt, wild-type. Scale bars = 100 μm.

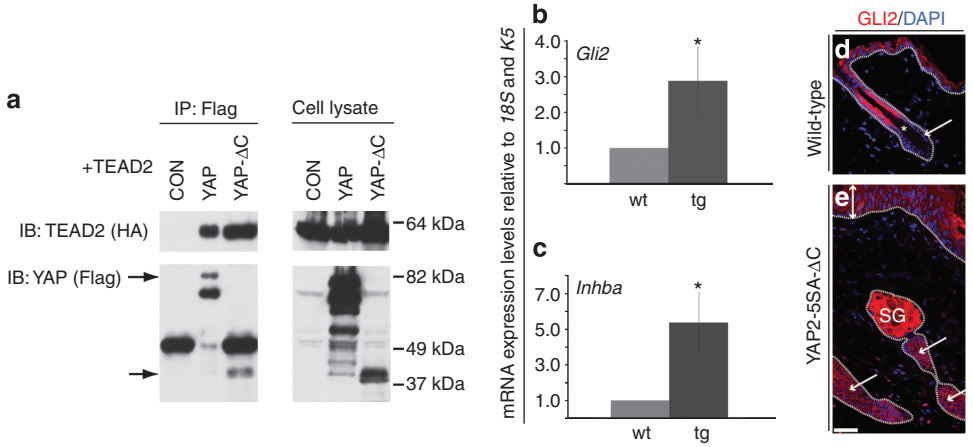

Figure 6. YAP lacking it C-terminus can still interact with TEAD transcription factors and activate transcription of target genes, *Gli2* and inhibin beta-A. (**a**) Immunoprecipitations with mouse anti-Flag agarose beads and rabbit anti-HA were used to detect HA-TEAD2, whereas mouse anti-Flag was used to detect YAP and YAP-ΔC. Top panel: equivalent amounts of TEAD2 were immunoprecipitated by YAP and YAP-ΔC. (**b**, **c**) y Axis displays relative fold expression levels with the expression levels in wild-type set to 1. Error bars represent SEM ($N=3$). Asterisks indicate statistically significant differences in gene expression levels ($P<0.05$). (**d**, **e**) GLI2 protein is expressed in hyperproliferative cells of YAP2-5SA-ΔC skin. Asterisks in **d** marks hair shaft. Double arrows in **e** highlight increased thickness of the interfollicular epidermis. Single arrows indicate location of the hair follicle bulge. Basement membranes are demarcated by dashed lines. CON, control; DAPI, 4′,6-diamidino-2-phenylindole; GLI2, glioma-associated oncogene family zinc finger 2; IB, immunoblot; Inhba, inhibin beta-A; IP, immunoprecipitation; SG, sebaceous gland; YAP, yes-associated protein. Scale bars = 100 μm.

epidermis (Schlegelmilch *et al.*, 2011). These data suggest that YAP2-5SA-ΔC may still retain its full capacity to bind TEAD cofactors through intact regions in the N-terminus and to activate target gene transcription and cell proliferation.

To test this hypothesis, we sought to determine whether deletion of the C-terminus of YAP affected its ability to complex with TEAD by conducting immunoprecipitation studies *in vitro*. HEK293 cells were cotransfected with HA-TEAD2 and either Flag-YAP, Flag-YAP-ΔC, or control plasmids. Cell lysates were incubated with mouse anti-Flag conjugated beads and immunoblotting was performed with rabbit anti-HA and anti-Flag antibodies. We found that TEAD2 interacted with both YAP and YAP-ΔC proteins with comparable affinity (top blot, Figure 6a), showing that even in the absence of its C-terminus, YAP can still interact with TEAD transcription factors.

To test whether YAP2-5SA-ΔC was still able to activate transcription of known YAP/TEAD target genes *in vivo*, we performed quantitative real-time reverse transcriptase–PCR assays to determine the relative expression levels of direct target genes of YAP/TEAD in *Keratin 5*-expressing cells in the epidermis of P85 wild-type and YAP2-5SA-ΔC transgenic mice. We found that the expression of the two target genes, glioma-associated oncogene family zinc finger 2 (*Gli2*) (Zhao *et al.*, 2008; Fernandez *et al.*, 2009) and Inhibin beta-A Zhang *et al.*, 2008a; Zhao *et al.*, 2008) were upregulated ~3-fold ($P<0.05$; $n=3$, Figure 6b) and 5-fold ($P<0.05$; $n=3$, Figure 6c), respectively. In addition, we detected GLI2 protein in the hyperproliferative stem/progenitor cells in the interfollicular epidermis and hair follicles of P85 YAP2-5SA-ΔC skin (Figure 6d and e).

These data, together with the observed increased cell proliferation rates in the epidermis of the YAP2-5SA-ΔC transgenic mice, lead us to conclude that the YAP/TEAD complex does not depend on YAP regions C-terminal of Q281 *in vivo* (including the YAP transactivation domain and a PDZ-binding motif) to activate the transcription of target genes, which control cell proliferation in epidermal stem/progenitor cell populations. Our conclusion is consistent with recent evidence that the *Drosophila melanogaster* YAP ortholog, Yorkie, which has a vastly disparate C-terminus, but highly conserved TEAD-binding and WW domains, is capable of driving tissue growth in *Drosophila melanogaster* and in mice (Dong *et al.*, 2007; Hilman and Gat, 2011). Moreover, a recent report shows that the C-termini of YAP and Yorkie are indeed dispensable for their ability to drive cell transformation *in vitro* and tissue growth *in vivo,* respectively (Zhang *et al.*, 2012).

In contrast to the reported loss of differentiated epidermal cell types in the interfollicular epidermis of YAPS127A transgenic mice (Schlegelmilch *et al.*, 2011; Zhang *et al.*, 2011a), we instead observed thickening of the spinous and granular cell layers, and hyperkeratinization in the interfollicular epidermis of postnatal YAP2-5SA-ΔC transgenic mice (Figure 4c–h). In addition, *Hes1* mRNA expression levels were unchanged in the skin of YAP2-5SA-ΔC transgenic mice compared with the wild-type mice (data not shown). In contrast, Zhang *et al.* (2011a) reported reduced HES1 expression levels in the interfollicular epidermis of YAPS127A transgenic mice, indicative of a reduced fate switch between undifferentiated basal progenitors and spinous cells. These results suggest that the C-terminus of YAP (from Q281) may control the balance between epidermal stem/progenitor cell proliferation and differentiation in the interfollicular epidermis.

In the YAP2-5SA-ΔC transgenic mice, hair follicles initially form and undergo first postnatal anagen relatively normally, but in subsequent stages, the K15/SOX9/LHX2/CD34-expressing hair follicle stem/progenitor bulge start to proliferate and form abnormal and massively expanded cell masses, which

fail to differentiate. Ultimately these defects lead to alopecia. Conceivably, this phenotype is caused by a failure to correctly respond to regulatory signals emanating from the dermal papilla. In contrast to the YAPS127A transgenic mice described by Zhang *et al.* (2011a), we did not observe signs of evaginating hair follicles at any stage in the postnatal YAP2-5SA-ΔC transgenic epidermis. This may be explained by the later onset of transgene expression, given no grossly abnormal epidermal phenotype was visible at around birth. The expression patterns of bulge stem/progenitor cell markers and the loss of hair follicle differentiation markers in YAP2-5SA-ΔC transgenic skin, however, were consistent with the reported expression of these markers in late embryonic and newborn YAPS127A transgenic hair follicles (Zhang *et al.*, 2011a).

In summary, we show that YAP functions independently of its C-terminal domain as a molecular switch to control epidermal stem/progenitor cell proliferation *in vivo*. YAP is now emerging as a potential therapeutic target for skin cancer, psoriasis, and degenerative skin diseases such as epidermolysis bullosa.

MATERIALS AND METHODS

Generation of transgenic mice

Protocols and use of animals in the described experiments were approved by the Animal Welfare Unit of the University of Queensland, which is registered as an institution that uses animals for scientific purposes under the Queensland Animal Care and Protection Act (2001). *Yap* complementary DNA encoding the mutant YAP2 protein ''YAP2-5SA-ΔC'' (provided by Professor Kun-Liang Guan) (Zhao *et al.*, 2007) was cloned into the *Nhe*I and *Sna*BI restriction sites of the transgenic vector containing 5.2 kb 5′-regulatory sequences of the bovine Keratin 5 gene (provided by Angel Ramirez (Ramirez *et al.*, 1994)). The 6.1 kb transgenic fragment was released using *Kpn*1 and microinjected into the pronuclei of zygotes of (C57Bl × CBA) F1 hybrid mice. Founders were identified by PCR genotyping of genomic tail DNA using forward primer 5′-TGGGCTGGGAAGGTGTCCATTTGC-3′ and reverse primer 5′-CACTGGTGTTGGGAGAAGCAGCA-3′ that amplify a 992 bp fragment unique to the pBK5-YAP transgenic vector. Founders were intercrossed with C57Bl mice for the generation of transgenic founder lines. Transgenic mice were creamed with Derisal daily, which reduced the skin lesions, but did not affect the phenotypic abnormalities.

Tissue preparation and embedding

Newborn and adult mice were killed by decapitation and cervical dislocation, respectively. Dorsal skin was dissected and immersion fixed for 15 hours at 4 °C in Tellyesniczky/Fekete solution (70% EtOH containing 5% glacial acetic acid and 10% formalin). Subsequently, tissue was dehydrated in EtOH and xylene series and processed for paraffin embedding using routine histology methods. Paraffin sections (8–10 μm) were cut, collected on Superfrost Plus glass slides, and stored at room temperature.

Histological staining, immunostaining, and alkaline phosphatase staining assays

Paraffin sections were first rehydrated and stained with haematoxylin/eosin using common histological staining protocols. Immunohistochemistry was performed as previously described (St John *et al.*, 2006). For immunofluoresence, sections were blocked in 2% BSA (Sigma Chemical Corporation, Castle Hill, NSW, Australia) in 0.1 M tris-buffered saline (pH 7.2) with 0.3% Triton-X-100 for 30 minutes at room temperature. The sections were incubated overnight at 4 °C with primary antibodies diluted in 2% BSA and 0.3% TX-100 in tris-buffered saline, washed with tris-buffered saline/Triton-X-100, and incubated with the appropriate secondary antibodies in the dark for 2 hours at room temperature. Sections were counterstained with 4′,6-diamidino-2-phenylindole and examined using an Olympus BX61 upright confocal microscope (Mt Waverley, VIC, Australia). The following antibodies were used: anti-Yap (1:200; Abcam ab39361, Waterloo, NSW, Australia), anti-Yap phospho S127 (1:100, Abcam ab76252), anti-Keratin 14 (1:1000; Covance PRB-155P, North Ride, NSW, Australia), anti-Keratin 10 (1:500; Covance PRB-159P), anti-involucrin (1:500; Covance PRB-140C), anti-loricrin (1:500; Covance PRB-145P), anti-Keratin 6 (1:200; Covance PRB-169P), anti-Keratin 15 (1:500; Covance PCK-153P), anti-SOX9 (1:100; Santa Cruz, Santa Cruz, CA, sc-20095), anti-LHX2 (1:50; Santa Cruz, sc-19344), anti-P63 (1:200; Santa Cruz sc-8343), anti-phospho-histon H3 (1:200; Millipore, Temecula, CA, 06-570), goat anti-P-Cadherin (1:50; R&D, Waterloo, NSW, Australia, Systems AF761), rat anti-CD34 (1:30, kindly provided by Prof. E. Dejana, IFOM, Milan, Italy), anti-GLI2 (1:100; Abcam ab7195), goat anti-Rabbit-Alexa 594 (1:200; Molecular Probes, Eugene, OR, A-11012), goat anti-Chicken-Alexa 594 (1:200; Molecular Probes A-11042), rabbit anti-rat Alexa 594 (1:200, Molecular Probes A-21211), and biotinylated goat anti-rabbit Ig antibodies (1:400, Vector Laboratories, Burlingame, CA).

For alkaline phosphatase staining, sections were incubated with the alkaline phosphatase substrate, nitro-blue tetrazolium chloride/5-bromo-4-chloro-3′-indolyphosphate p-toluidine salt (Roche), for 30 minutes at room temperature and counterstained with Nuclear Fast Red solution (Sigma, Castle Hill, NSW, Australia).

Immunoprecipitation and immunoblotting

Immunoprecipitation and immunoblotting were performed as described previously (Zhang *et al.*, 2009). Briefly, Flag-YAP, Flag-YAP-ΔC (Zhang *et al.*, 2012), or control empty vector plasmids were transfected into HEK-293T cells, together with HA-tagged TEAD2. Cells were lysed after 48 hours and immunoprecipitated with anti-Flag agarose beads (Sigma). Immunoprecipitates were separated by sodium dodecyl sulfate-polyacrylamide gel electrophoresis and immunoblotted with anti-Flag (Sigma) or anti-HA (Santa Cruz).

Quantitative real-time PCR assays

Total RNA was extracted from dissected P85 using the RNeasy Mini kit (QIAGEN, Chadstone Centre, VIC, Australia) according to the manufacturer's instructions, including on-column DNase digestion. Total RNA was reverse-transcribed with random primers (Promega, South Sydney, NSW, Australia) and Superscript III (Invitrogen, Carlsbad, CA) using standard methodologies. Quantitative real-time reverse transcriptase–PCR primers were designed with melting temperature (Tm) of close to 60 °C to generate 60–145 bp amplicons: *Gli2*-F: 5′-GCAGACTGCACCAAGGAGTA-3′, *Gli2*-R: 5′-CGTGGATGTGTTCATTGTTGA-3′, Inhibin beta-A-F: 5′-ATCATCACCTTTGCCGAGTC-3′, Inhibin beta-A-R: 5′-TCACTGCCTTCCTTGGAAAT-3′, *Keratin 5*-F: 5′-CAGAGCTGAGGAACATGCAG-3′, *Keratin 5*-R: 5′CA

TTCTCAGCCGTGGTACG-3′, *AE13*-F: 5′-CCATTGAAGAACTCCAA CAAAA-3′, *AE13*-R: 5′-GCAGTTGTCCACCTGAACG-3′, *AE15*-F: 5′-GAGCTAAGACGCGAGCAAGA-3′, *AE15*-R: 5′-CCACCTCTGGGTA ATGCTCT-3′, *Lef1*-F: 5′-TCCTGAAATCCCCACCTTCT-3′, *Lef1*-R: 5′-TGGGATAAACAGGCTGACCT-3′, *Msx2*-F: 5′-AGGAGCCCGGCA GATACT-3′, *Msx2*-R: 5′-GTTTCCTCAGGGTGCAGGT-3′, *18S*-F: 5′-GATCCATTGGAGGGCAAGTCT-3′, *18S*-R: 5′-CCAAGATCCAACTA CGAGCTTTTT-3′. Quantitative real-time reverse transcriptase–PCR assays were carried out using SYBR green PCR master mix and an ABI PRISM 7500 Sequence Detection System. Target complementary DNA levels were analyzed by the comparative cycle time method and values were normalized to *18S* ribosomal RNA expression levels. Statistical significance of changes in relative gene expression was assessed by a Student's paired *t*-test with a one-tailed distribution.

CONFLICT OF INTEREST

The authors state no conflict of interest.

ACKNOWLEDGMENTS

We thank Ms Julie Conway for mouse colony management, Prof. Kun-Liang Guan and Dr Bin Zhao (University of California, San Diego, USA), Dr Angel Ramirez and Dr J.L. Jorcano (CIEMAT, Madrid, Spain) and Prof. Elisabetta Dejana (IFOM, Milan, Italy) for provision of reagents, and Dr Christelle Adolphe (The University of Queensland) for stimulating and insightful discussions. This work was supported by the National Health and Medical Research Council of Australia.

REFERENCES

Camargo FD, Gokhale S, Johnnidis JB *et al.* (2007) YAP1 increases organ size and expands undifferentiated progenitor cells. *Curr Biol* 17:2054–60

Chan SW, Lim CJ, Chen L *et al.* (2011) The Hippo pathway in biological control and cancer development. *J Cell Physiol* 226:928–39

Chase HB, Rauch R, Smith VW (1951) Critical stages of hair development and pigmentation in the mouse. *Physiol Zool* 24:1–8

Dong J, Feldmann G, Huang J *et al.* (2007) Elucidation of a universal size-control mechanism in Drosophila and mammals. *Cell* 130:1120–33

Fernandez LA, Northcott PA, Dalton J *et al.* (2009) YAP1 is amplified and up-regulated in hedgehog-associated medulloblastomas and mediates Sonic hedgehog-driven neural precursor proliferation. *Genes Dev* 23:2729–41

Fuchs E, Green H (1980) Changes in keratin gene expression during terminal differentiation of the keratinocyte. *Cell* 19:1033–42

Gat U, DasGupta R, Degenstein L *et al.* (1998) *De Novo* hair follicle morphogenesis and hair tumors in mice expressing a truncated beta-catenin in skin. *Cell* 95:605–14

Greco V, Chen T, Rendl M *et al.* (2009) A two-step mechanism for stem cell activation during hair regeneration. *Cell Stem Cell* 4:155–69

Hall CA, Wang R, Miao J *et al.* (2010) Hippo pathway effector Yap is an ovarian cancer oncogene. *Cancer Res* 70:8517–25

Hans F, Dimitrov S (2001) Histone H3 phosphorylation and cell division. *Oncogene* 20:3021–7

Harvey K, Tapon N (2007) The Salvador-Warts-Hippo pathway - an emerging tumour-suppressor network. *Nat Rev Cancer* 7:182–91

Hilman D, Gat U (2011) The evolutionary history of YAP and the hippo/YAP pathway. *Mol Biol Evol* 28:2403–17

Hoshino M, Qi ML, Yoshimura N *et al.* (2006) Transcriptional repression induces a slowly progressive atypical neuronal death associated with changes of YAP isoforms and p73. *J Cell Biol* 172:589–604

Ito M, Kizawa K, Hamada K *et al.* (2004) Hair follicle stem cells in the lower bulge form the secondary germ, a biochemically distinct but functionally equivalent progenitor cell population, at the termination of catagen. *Differentiation* 72:548–57

Liu Y, Lyle S, Yang Z *et al.* (2003) Keratin 15 promoter targets putative epithelial stem cells in the hair follicle bulge. *J Invest Dermatol* 121:963–8

Lo Celso C, Prowse DM, Watt FM (2004) Transient activation of beta-catenin signalling in adult mouse epidermis is sufficient to induce new hair follicles but continuous activation is required to maintain hair follicle tumours. *Development* 131:1787–99

Lowry WE, Blanpain C, Nowak JA *et al.* (2005) Defining the impact of beta-catenin/Tcf transactivation on epithelial stem cells. *Genes Dev* 19:1596–611

Lu L, Li Y, Kim SM *et al.* (2010) Hippo signaling is a potent *in vivo* growth and tumor suppressor pathway in the mammalian liver. *Proc Natl Acad Sci USA* 107:1437–42

Muller-Rover S, Tokura Y, Welker P *et al.* (1999) E- and P-cadherin expression during murine hair follicle morphogenesis and cycling. *Exp Dermatol* 8:237–46

Ota M, Sasaki H (2008) Mammalian tead proteins regulate cell proliferation and contact inhibition as transcriptional mediators of Hippo signaling. *Development* 135:4059–69

Panteleyev AA, Jahoda CA, Christiano AM (2001) Hair follicle predetermination. *J Cell Sci* 114:3419–31

Ramalho-Santos M, Yoon S, Matsuzaki Y *et al.* (2002) ''Stemness'': transcriptional profiling of embryonic and adult stem cells. *Science* 298:597–600

Ramirez A, Bravo A, Jorcano JL *et al.* (1994) Sequences 5′ of the bovine keratin 5 gene direct tissue- and cell-type-specific expression of a lacZ gene in the adult and during development. *Differentiation* 58:53–64

Reginelli AD, Wang YQ, Sassoon D *et al.* (1995) Digit tip regeneration correlates with regions of Msx1 (Hox 7) expression in fetal and newborn mice. *Development* 121:1065–76

Rendl M, Polak L, Fuchs E (2008) BMP signaling in dermal papilla cells is required for their hair follicle-inductive properties. *Genes Dev* 22:543–57

Rhee H, Polak L, Fuchs E (2006) Lhx2 maintains stem cell character in hair follicles. *Science* 312:1946–9

Schlegelmilch K, Mohseni M, Kirak O *et al.* (2011) Yap1 acts downstream of alpha-catenin to control epidermal proliferation. *Cell* 144:782–95

Schmidt-Ullrich R, Paus R (2005) Molecular principles of hair follicle induction and morphogenesis. *Bioessays* 27:247–61

Song H, Mak KK, Topol L *et al.* (2010) Mammalian Mst1 and Mst2 kinases play essential roles in organ size control and tumor suppression. *Proc Natl Acad Sci USA* 107:1431–6

St John JA, Claxton C, Robinson MW *et al.* (2006) Genetic manipulation of blood group carbohydrates alters development and pathfinding of primary sensory axons of the olfactory systems. *Dev Biol* 298:470–84

Trempus CS, Morris RJ, Bortner CD *et al.* (2003) Enrichment for living murine keratinocytes from the hair follicle bulge with the cell surface marker CD34. *J Invest Dermatol* 120:501–11

Van Mater D, Kolligs FT, Dlugosz AA *et al.* (2003) Transient activation of beta -catenin signaling in cutaneous keratinocytes is sufficient to trigger the active growth phase of the hair cycle in mice. *Genes Dev* 17:1219–24

Vidal VP, Chaboissier MC, Lutzkendorf S *et al.* (2005) Sox9 is essential for outer root sheath differentiation and the formation of the hair stem cell compartment. *Curr Biol* 15:1340–51

Wang Y, Dong Q, Zhang Q *et al.* (2010) Overexpression of yes-associated protein contributes to progression and poor prognosis of non-small-cell lung cancer. *Cancer Sci* 101:1279–85

Winter H, Langbein L, Praetzel S *et al.* (1998) A novel human type II cytokeratin, K6hf, specifically expressed in the companion layer of the hair follicle. *J Invest Dermatol* 111:955–62

Wu S, Liu Y, Zheng Y *et al.* (2008) The TEAD/TEF family protein Scalloped mediates transcriptional output of the Hippo growth-regulatory pathway. *Dev Cell* 14:388–98

Xu MZ, Yao TJ, Lee NP *et al.* (2009) Yes-associated protein is an independent prognostic marker in hepatocellular carcinoma. *Cancer* 115:4576–85

Zhang H, Pasolli HA, Fuchs E (2011a) Yes-associated protein (YAP) transcriptional coactivator functions in balancing growth and differentiation in skin. *Proc Natl Acad Sci USA* 108:2270–5

Zhang J, Smolen GA, Haber DA (2008a) Negative regulation of YAP by LATS1 underscores evolutionary conservation of the *Drosophila Hippo* pathway. *Cancer Res* 68:2789–94

Zhang L, Ren F, Zhang Q *et al.* (2008b) The TEAD/TEF family of transcription factor Scalloped mediates Hippo signaling in organ size control. *Dev Cell* 14:377–87

Zhang X, George J, Deb S *et al.* (2011b) The Hippo pathway transcriptional co-activator, YAP, is an ovarian cancer oncogene. *Oncogene* 30:2810–22

Zhang X, Grusche FA, Harvey KF (2012) Control of tissue growth and cell transformation by the Salvador/Warts/Hippo pathway. *PLoS One* 7:e31994

Zhang X, Milton CC, Humbert PO *et al.* (2009) Transcriptional output of the Salvador/warts/hippo pathway is controlled in distinct fashions in *Drosophila melanogaster* and mammalian cell lines. *Cancer Res* 69:6033–41

Zhang Y, Andl T, Yang SH *et al.* (2008c) Activation of beta-catenin signaling programs embryonic epidermis to hair follicle fate. *Development* 135:2161–72

Zhao B, Wei X, Li W *et al.* (2007) Inactivation of YAP oncoprotein by the Hippo pathway is involved in cell contact inhibition and tissue growth control. *Genes Dev* 21:2747–61

Zhao B, Ye X, Yu J *et al.* (2008) TEAD mediates YAP-dependent gene induction and growth control. *Genes Dev* 22:1962–71

Zhou D, Conrad C, Xia F *et al.* (2009) Mst1 and Mst2 maintain hepatocyte quiescence and suppress hepatocellular carcinoma development through inactivation of the Yap1 oncogene. *Cancer Cell* 16:425–38

Zhou D, Zhang Y, Wu H *et al.* (2011) Mst1 and Mst2 protein kinases restrain intestinal stem cell proliferation and colonic tumorigenesis by inhibition of Yes-associated protein (Yap) overabundance. *Proc Natl Acad Sci USA* 108:E1312–20

Zhou P, Byrne C, Jacobs J *et al.* (1995) Lymphoid enhancer factor 1 directs hair follicle patterning and epithelial cell fate. *Genes Dev* 9:700–13